Title

Automated algorithm for counting microbleeds in patients with familial cerebral cavernous malformations

Journal

Neuroradiology, 59(7)

ISSN

0028-3940

Authors

Zou, Xiaowei
Hart, Blaine L
Mabray, Marc
et al.

Publication Date

2017-07-01

DOI

10.1007/s00234-017-1845-8

Peer reviewed

HHS Public Access

Author manuscript

Neuroradiology. Author manuscript; available in PMC 2018 July 01.

Published in final edited form as:

Neuroradiology. 2017 July ; 59(7): 685–690. doi:10.1007/s00234-017-1845-8.

Automated algorithm for counting microbleeds in patients with familial cerebral cavernous malformations

Xiaowei Zou, PhD[1], **Blaine L. Hart, MD**[2], **Marc Mabray, MD**[2], **Mary R. Bartlett, BS**[3], **Wei Bian, PhD**[4], **Jeffrey Nelson, MS**[5], **Leslie A. Morrison, MD**[3], **Charles E. McCulloch, PhD**[6], **Christopher P. Hess, MD, PhD**[1], **Janine M. Lupo, PhD**[1], and **Helen Kim, PhD**[5,6,*]

[1]Department of Radiology and Biomedical Imaging, University of California, San Francisco, 505 Parnassus Avenue, M-391, San Francisco, California 94143-0628, USA

[2]Department of Radiology, University of New Mexico, MSC 10 5530, 1 University of New Mexico, Albuquerque, New Mexico 87131, USA

[3]Department of Neurology, University of New Mexico, MSC 10 5620, Health Sciences Center, 1 University of New Mexico, Albuquerque, New Mexico 87131-0001, USA

[4]Department of Radiology, Stanford University, 300 Pasteur Drive, Stanford, California 94305-5105, USA

[5]Department of Anesthesia and Perioperative Care, Center for Cerebrovascular Research, University of California, San Francisco, 1001 Potrero Avenue, Box 1363, San Francisco, California 94143, USA

[6]Department of Epidemiology and Biostatistics, University of California, San Francisco, 550 16th Street, 2nd Floor, San Francisco, California 94158-2549, USA

Abstract

Introduction—Familial cerebral cavernous malformation (CCM) patients present with multiple lesions that can grow both in number and size over time and are reliably detected on susceptibility-weighted imaging (SWI). Manual counting of lesions is arduous and subject to high variability.

[*]**Address correspondence to:** Helen Kim, PhD, Department of Anesthesia and Perioperative Care, University of California, San Francisco, 1001 Potrero Avenue, Box 1363, San Francisco, CA 94143, Phone: 415-206-4789, Fax: 415-206-8907, Helen.Kim2@ucsf.edu.

Conflict of Interest

The authors declare that they have no conflict of interest.

Ethical Approval

We declare that all human studies have been approved by the institutional review board of the University of New Mexico and have therefore been performed in accordance with the ethical standards laid down in the 1964 Declaration of Helsinki and its later amendments.

Informed Consent

We declare that all patients gave informed consent prior to inclusion in this study.

Author Contributions

X Zou: Project development, Data analysis, Manuscript writing and editing; BL Hart: Project development, Data collection, Manuscript editing; M Mabray: Data collection, Manuscript editing; MR Barlett: Data collection; W Bian: Algorithm development, Manuscript editing; J Nelson: Statistical analysis, Manuscript editing; LA Morrison: Project development, Data collection, Manuscript editing; CE McCulloch: Statistical analysis, Manuscript editing; CP Hess: Project development, Manuscript editing; JM Lupo: Project development, Manuscript editing; H Kim: Project development, Manuscript writing and editing

We aimed to develop an automated algorithm for counting CCM microbleeds (lesions <5mm in diameter) on SWI images.

Methods—Fifty-seven familial CCM type-1 patients were included in this institutional review board-approved study. Baseline SWI (n=57) and follow-up SWI (n=17) were performed on a 3T Siemens MR scanner with lesions counted manually by the study neuroradiologist. We modified an algorithm for detecting radiation-induced microbleeds on SWI images in brain tumor patients, using a training set of 22 manually delineated CCM microbleeds from 2 random scans. Manual and automated counts were compared using linear regression with robust standard errors, intra-class correlation (ICC), and paired t-tests. A validation analysis comparing the automated counting algorithm and a consensus read from two neuroradiologists was used to calculate sensitivity, the proportion of microbleeds correctly identified by the automated algorithm.

Results—Automated and manual microbleed counts were in strong agreement in both baseline (ICC=0.95, p<0.001) and longitudinal (ICC=0.88, p<0.001) analyses, with no significant difference between average counts (baseline p=0.11, longitudinal p=0.29). In the validation analysis, the algorithm correctly identified 662 of 1325 microbleeds (sensitivity=50%), again with strong agreement between approaches (ICC=0.77, p<0.001).

Conclusion—The automated algorithm is a consistent method for counting microbleeds in familial CCM patients that can facilitate lesion quantification and tracking.

Keywords

Automated lesion counting; Cerebral cavernous malformations; Microbleeds; Susceptibility-weighted imaging

Introduction

Cerebral cavernous malformations (CCM) are clusters of abnormally enlarged, leaky capillary caverns that occur primarily in the brain and spinal cord, with an estimated prevalence of 0.1–0.5% in the general population [1]. Common clinical manifestations of CCM include seizures (50%), cerebral hemorrhage (25%), and focal neurological deficits (25%) [2]. CCM can occur in a sporadic form or in a familial form with autosomal dominant inheritance (10–50%) [3]. Familial CCM cases often present with multiple lesions that can be visualized on magnetic resonance imaging as foci of low signal intensity on T2*-weighted imaging or susceptibility-weighted imaging (SWI). Both the number and size of lesions in patients with familial CCM increase with advancing age [4].

The number of CCM lesions correlates with increased expression of angiogenic and growth factors [5], and thus has been used as a surrogate biomarker for CCM disease severity in several studies [1, 6, 7]. Clinical diagnostic imaging reports often note new lesions, acute hemorrhage and edema, and the presence of multiple lesions, which does not fully illustrate the magnitude of the problem. Furthermore, change in the number of lesions could potentially be used to monitor disease progression in longitudinal studies. Large CCM lesions are easily identified upon manual examination. However, manual counting of small CCM lesions (< 5mm in diameter), hereafter referred to as microbleeds, in patients with familial CCM is an arduous task because of the large number of lesions (~50 lesions on

average for adults), the lengthy counting time (20–90 minutes per case), and the high intra- and inter-rater variability [8, 9]. Thus, application of an automated counting algorithm for microbleeds in patients with familial CCM would be highly desirable.

Several automated algorithms have been proposed to detect microbleeds on SWI images in various populations, including Alzheimer's disease [10], atherosclerotic disease [11], stroke [12, 13], traumatic brain injury [14], and brain tumors [15]. These algorithms can be divided into two categories: hypothesis-driven approaches that are based on pre-defined geographic features (such as shape and size) and data-driven approaches that are based on extracted high-level features. In general, hypothesis-driven approaches [11, 12, 14, 15] are relatively simple to implement, but rely on limited known physical features of microbleeds. On the other hand, data-driven approaches [10, 13]can extract hundreds and thousands of high-level features but place higher demands on the computational resources required and may come with the risk of over-fitting.

In this study, we sought to adapt and modify a simple microbleed detection algorithm for counting CCM microbleeds on SWI images in patients with familial CCM. Our goal was to develop an automated counting algorithm with minimal false positives that would yield approximately equivalent microbleed counts to manual microbleed counts by experienced neuroradiologists to facilitate lesion quantification and tracking in familial CCM.

Materials and Methods

Patients and MRI scans

For this study, we included 57 familial CCM type-1 patients with the common Hispanic mutation (CCM1-CHM) who were enrolled in the ongoing Brain Vascular Malformation Consortium (BVMC) CCM study (Table 1) [6]. All patients had baseline SWI scans and 17 had follow-up SWI scans, all performed on a 3T Siemens MR scanner. The imaging parameters of the SWI sequence were: in-plane FOV = 25.6 × 19.2 cm, in-plane resolution = 1.0 × 1.0 mm, axial slice thickness = 1.5 mm, number of slices = 88, flip angle = 15°, pixel bandwidth = 120 Hz, TE = 20 ms, TR = 28 ms, parallel imaging factor = 2, and total scan time = 4:55 minutes. All participants provided written informed consent, and the study was approved by the local institutional review board.

Manual assessment of microbleeds

An experienced neuroradiologist (BH), who was blinded to the results of the automated algorithm, manually counted the total number of lesions and the number of large lesions (≥ 5mm in diameter) on SWI images of all scans. Microbleeds are defined here as CCM lesions < 5mm in diameter and are derived as the difference between total lesion count and number of large lesions. The neuroradiologist manually delineated the location of 22 microbleeds on SWI images of two random scans in order to train the algorithm.

Automated algorithm development

We adapted and modified an existing automated algorithm [15] for detecting CCM microbleeds (Fig. 1) in the MATLAB environment (MathWorks, Natick, MA). The

algorithm was applied to minimum-intensity-projected SWI images (6-mm projection thickness) after brain extraction. The algorithm identified potential microbleeds using a 2-dimensional fast radial symmetry transform (2D-FRST) based on local intensity gradients, where n was number of radii, α was the degree of circularity, prctTH was the percentile threshold of image gradient magnitude, and minVesArea was the minimum number of pixels any vessel region should contain. The algorithm then screened each voxel using multiple thresholds of 2D-FRST values (lowerTH1, lowerTH2, upperTH) and removed false positives via vessel masking and examination of geometric features after 3-dimensional region growing.

When the original algorithm [15] was applied to 8 scans from CCM1-CHM patients, over 100 false positives were identified per scan. In one scan, the original automated algorithm counted 150 microbleeds where the manual count was 22. In another scan, the original automated algorithm counted 96 microbleeds where the manual count was 8. Moreover, the automated counts of the other six scans which the radiologist had identified with zero lesions were 121, 120, 108, 12, 127, and 107. Therefore, we used 22 delineated microbleeds from two randomly-selected scans of CCM1-CHM patients as a training set to empirically determine the algorithm parameters with the goal of reducing the number of false positives while maintaining high sensitivity. Since CCM microbleeds are larger and less spherical in shape than radiation-induced microbleeds and the voxel size of the SWI images differed, our strategy was to appropriately modify variables that initially defined the radial symmetry transform and then determined thresholds for segmenting the resulting output mask. This approach allowed for larger microbleeds with less circularity to be captured in the initial detection step and not subsequently removed while reducing false positives. The final parameters were: n = 3, α = 3, prctTH = 90, minVesArea = 25, lowerTH1 = 45, lowerTH2 = 65, upperTH = 170. Potential microbleeds within 3mm from the edge of brain were also removed to further reduce false positives.

Validation dataset

Because there is no gold standard for CCM lesion counting, we generated a validation dataset on which two neuroradiologists (BH and MM) reviewed and delineated microbleeds for a selected single slice (slice 50 ± 2 slices on either side for review) independent of each other for 47 baseline scans. These manual counts were then reviewed by consensus reading and compared to counts generated by the automated algorithm to determine sensitivity.

Statistical analysis

For the training set of 22 microbleeds in two random scans, false positives (number of microbleeds incorrectly counted by automated algorithm), and false negatives (number of microbleeds not detected by the automated algorithm) were reported. The manual and automated microbleed counts were compared using linear regression with robust standard errors to accommodate heteroskedasticity, intra-class correlation, and paired t-test. The sensitivity (proportion of microbleeds correctly identified by the automated algorithm), false negative rate, linear regression R^2, and intra-class correlation based on automated and consensus counts in the validation dataset are reported.

Results

Training scans

For the training set in two random scans, the modified automated algorithm missed 3 out of 22 microbleeds, and identified an additional 34 microbleeds that were not counted by the neuroradiologist. Two of the false negatives were small microbleeds with very low contrast, while the third false negative had slightly shifted center across slices (Fig. 2a). Most of the false positives were ending, cross-section, or turning points of vessels, and a few false positives were thought to be due to SWI artifacts (Fig. 2b).

Baseline scans

In the 57 baseline scans, manual microbleed counts ranged from 0 to 617, whereas the automated counts ranged from 11 to 715 (Fig. 3). The computation time for the automated algorithm was approximately 1 minute per patient on a one-core Linux workstation with Intel Core 2 Extreme CPU X9650 quad processors at 3.0 GHz and 8 GB RAM. There was a significant linear relationship between automated and manual counts ($R^2 = 0.90$, $p < 0.001$). The high intra-class correlation coefficient (ICC = 0.95, 95% CI = 0.91 – 0.97, $p < 0.001$) suggested that the two counting methods had high agreement. No statistically significant difference was found between the difference of the means of the manual and automated counts ($p = 0.11$, 95% CI = −25.2 – 2.6, paired t-test).

Longitudinal scans

The time interval between baseline and follow-up scans was 39.4 ± 5.3 months. The longitudinal change ranged from –11 to 97 in the manual counts (four negatives) and from −10 to 87 (four negatives) in the automated counts (Fig. 4). The four negative manual counts and the four negative automated counts did not occur in the same patients. A significant linear relationship ($R^2 = 0.77$, $p < 0.001$) and intra-class correlation (ICC = 0.88, 95% CI = 0.70 – 0.95, $p < 0.001$) were found in longitudinal changes in microbleed counts between manual and automated assessment, also with no statistically significant difference between the difference of their means ($p = 0.29$, 95% CI = −10.9 – 3.49, paired t-test).

Validation analysis

There was high pairwise correlation in counts (>0.95) between the two neuroradiologists and between each neuroradiologist and the algorithm (data not shown). A total of 1,325 microbleeds were identified by consensus review of 47 scans by the two neuroradiologists. The algorithm correctly identified 662 of these microbleeds (sensitivity = 0.50), and identified 40 false positives with a median of 1 false positive per observation (and a maximum of 8). The majority of these false positives (31/40) were determined to be vessels, most likely veins. There was a strong positive linear relationship ($R^2 = 0.94$, $p<0.001$) between consensus counts and automated counts; the intra-class correlation was 0.77 (95% CI = 0.62 – 0.87, $p<0.001$), suggesting moderate agreement (Fig. 5). The difference of the means of the consensus and automated counts was statistically different ($p<0.001$, 95% CI = 9.0 – 17.5, paired t-test), indicating that overall the consensus counts tended to be higher than the automated counts.

Discussion

In this study, we developed an automated algorithm for counting microbleeds in patients with familial CCM by modifying an existing algorithm. We found that the number of microbleeds counted by our algorithm was significantly correlated with the number counted manually by an experienced neuroradiologist in both baseline and longitudinal analyses, and by consensus reading of two neuroradiologists in validation analysis. On average, the automated algorithm (1 minute per patient) was 50 times faster than manual counting (50 minutes per patient) and was internally consistent.

A challenging feature of automating CCM lesion counts is their irregular appearance and size due to the pathology of disease, resulting in lesions filled with blood and lined with sinusoidal endothelium. These lesions also have varying intensity patterns, such as heterogeneous reticulated intensity or central high intensity surrounded by low signal [16]. In this study, the original algorithm generated over 100 false positives per scan and we empirically determined the algorithm parameters with the goal of reducing the number of false positives while maintaining a reasonable sensitivity, so that the automated counts would be approximately in the same range as compared to the manual counts. The technical advance of this algorithm was a significant reduction in the false positive rate for application to familial CCM. In a validation dataset of 47 scans with consensus reads by two neuroradiologists, the sensitivity of the automated algorithm was 50%, which may be due to increased reading sensitivity in the validation dataset compared with the training dataset as the neuroradiologists reported afterwards. However, given the significant correlation and high agreement between the number of microbleeds counted by the algorithm and by the neuroradiologists, our modified automated algorithm shows promise as an alternative method to manual microbleed counting, greatly facilitating lesion quantification and tracking for future clinical research studies.

A limitation of the current analysis was that the location of the manually counted microbleeds was not recorded in detail for all scans due to the large number of lesions. There is also no gold standard for manual counting of microbleeds in familial CCM for comparison. Thus, we performed a validation dataset in which microbleed counts from the automated algorithm were compared to consensus reads by two neuroradiologists to determine sensitivity. Automated counts reported in this study consisted of both true positives and false positives. In our validation analysis, the false positives identified by the algorithm were mostly due to structural features in which the neuroradiologists determined the potential microbleed to be vessels. This suggests that the number of false positives from the automated algorithm would be similar in both baseline and follow-up scans from the same patient and that any changes observed in longitudinal automated counts would reflect real differences. The few negative longitudinal changes from both manual and automated counts were likely due to random counting error, although resorption of acute hemorrhage may result in decreased size of some CCM lesions over time. The wide range of longitudinal changes observed over a relatively narrow time interval also suggests that the longitudinal change may not only be a function of time but also a function of faster disease progression in familial CCM1-CHM patients. Future studies will require further modifications to the algorithm and validation to determine the algorithm’s sensitivity.

In summary, our automated counting algorithm is an inherently consistent method for counting microbleeds in patients with familial CCM that could facilitate lesion quantification and tracking in clinical research studies, and raises clinical awareness for more vigilant imaging surveillance in patients with high number of microbleeds.

Acknowledgments

Funding

This work was supported by a Brain Vascular Malformation Consortium (BVMC) postdoctoral training fellowship to XZ as part of National Institutes of Health (NIH) grant U54 NS065705. The BVMC is a part of the NIH Rare Diseases Clinical Research Network (RDCRN), an initiative of the Office of Rare Diseases Research (ORDR) and the National Center for Advancing Translational Science (NCATS). The consortium is funded through collaboration between NCATS and the National Institute of Neurological Disorders and Stroke (NINDS). The scientific computing resources in this study were provided by the Department of Radiology, University of California, San Francisco, and supported by NIH P01 CA118816. We would like to thank Dr. Sarah J. Nelson for her valuable advice on study development.

References

1. Choquet H, Pawlikowska L, Lawton MT, Kim H. Genetics of cerebral cavernous malformations: current status and future prospects. J Neurosurg Sci. 2015; 59(3):211–220. [PubMed: 25900426]
2. Al-Shahi Salman R, Hall JM, Horne MA, Moultrie F, Josephson CB, Bhattacharya JJ, Counsell CE, Murray GD, Papanastassiou V, Ritchie V, Roberts RC, Sellar RJ, Warlow CP. Untreated clinical course of cerebral cavernous malformations: a prospective, population-based cohort study. Lancet Neurol. 2012; 11(3):217–224. [PubMed: 22297119]
3. Rigamonti D, Hadley MN, Drayer BP, Johnson PC, Hoenig-Rigamonti K, Knight JT, Spetzler RF. Cerebral cavernous malformations. Incidence and familial occurrence. N Engl J Med. 1988; 319(6): 343–347. [PubMed: 3393196]
4. Denier C, Labauge P, Bergametti F, Marchelli F, Riant F, Arnoult M, Maciazek J, Vicaut E, Brunereau L, Tournier-Lasserve E. Genotype-phenotype correlations in cerebral cavernous malformations patients. Ann Neurol. 2006; 60(5):550–556. [PubMed: 17041941]
5. Maiuri F, Cappabianca P, Gangemi M, De Caro Mdel B, Esposito F, Pettinato G, de Divitiis O, Mignogna C, Strazzullo V, de Divitiis E. Clinical progression and familial occurrence of cerebral cavernous angiomas: the role of angiogenic and growth factors. Neurosurg Focus. 2006; 21(1):e3.
6. Choquet H, Nelson J, Pawlikowska L, McCulloch CE, Akers A, Baca B, Khan Y, Hart B, Morrison L, Kim H. Association of cardiovascular risk factors with disease severity in cerebral cavernous malformations type 1 subjects with the common Hispanic mutation. Cerebrovasc Dis. 2014; 37(1): 57–63. [PubMed: 24401931]
7. Shenkar R, Shi C, Rebeiz T, Stockton RA, McDonald DA, Mikati AG, Zhang L, Austin C, Akers AL, Gallione CJ, Rorrer A, Gunel M, Min W, Marcondes de Souza J, Lee C, Marchuk DA, Awad IA. Exceptional aggressiveness of cerebral cavernous malformation disease associated with PDCD10 mutations. Genet Med. 2015; 17(3):188–196. [PubMed: 25122144]
8. Cordonnier C, Potter GM, Jackson CA, Doubal F, Keir S, Sudlow CL, Wardlaw JM, Al-Shahi Salman R. Improving interrater agreement about brain microbleeds: development of the Brain Observer MicroBleed Scale (BOMBS). Stroke. 2009; 40(1):94–99. [PubMed: 19008468]
9. Gregoire SM, Chaudhary UJ, Brown MM, Yousry TA, Kallis C, Jager HR, Werring DJ. The Microbleed Anatomical Rating Scale (MARS): reliability of a tool to map brain microbleeds. Neurology. 2009; 73(21):1759–1766. [PubMed: 19933977]
10. Barnes SR, Haacke EM, Ayaz M, Boikov AS, Kirsch W, Kido D. Semiautomated detection of cerebral microbleeds in magnetic resonance images. Magn Reson Imag. 2011; 29(6):844–852.
11. Kuijf HJ, de Bresser J, Geerlings MI, Conijn MM, Viergever MA, Biessels GJ, Vincken KL. Efficient detection of cerebral microbleeds on 7.0 T MR images using the radial symmetry transform. Neuroimage. 2012; 59(3):2266–2273. [PubMed: 21985903]

12. Seghier ML, Kolanko MA, Leff AP, Jager HR, Gregoire SM, Werring DJ. Microbleed detection using automated segmentation (MIDAS): a new method applicable to standard clinical MR images. PloS One. 2011; 6(3):e17547. [PubMed: 21448456]
13. Qi D, Hao C, Lequan Y, Lei Z, Jing Q, Defeng W, Mok VC, Lin S, Pheng-Ann H. Automatic detection of cerebral microbleeds from MR images via 3D convolutional neural networks. IEEE Trans Med Imaging. 2016; 35(5):1182–1195. [PubMed: 26886975]
14. van den Heuvel TL, van der Eerden AW, Manniesing R, Ghafoorian M, Tan T, Andriessen TM, Vande Vyvere T, van den Hauwe L, Ter Haar Romeny BM, Goraj BM, Platel B. Automated detection of cerebral microbleeds in patients with Traumatic Brain Injury. Neuroimage Clin. 2016:12241–251.
15. Bian W, Hess CP, Chang SM, Nelson SJ, Lupo JM. Computer-aided detection of radiation-induced cerebral microbleeds on susceptibility-weighted MR images. Neuroimage Clin. 2013:2282–290.
16. Kattapong VJ, Hart BL, Davis LE. Familial cerebral cavernous angiomas: clinical and radiologic studies. Neurology. 1995; 45(3 Pt 1):492–497. [PubMed: 7898703]

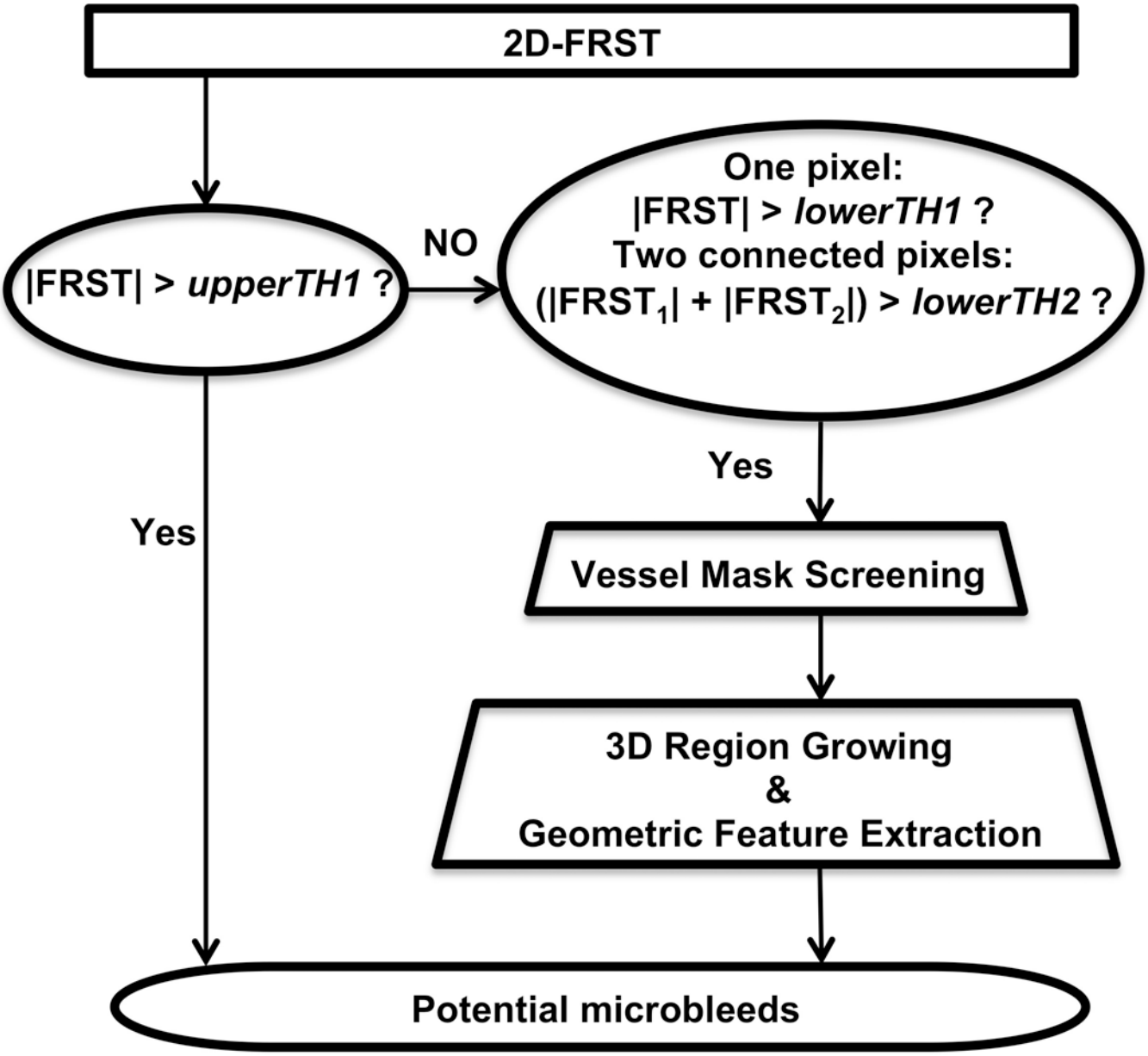

Fig. 1. Schematic flowchart of the automated algorithm

The algorithm appraises the spherical shape of microbleeds by applying a two-dimensional fast radial symmetry transform (2D-FRST). The higher the FRST value, the more circular the geometry. Pixels with FRST values higher than the threshold *upperTH1* are directly considered to be potential microbleeds. Other voxels selected by thresholds *lowerTH1* and *lowerTH2* will undergo vessel mask screening, three-dimensional region growing, and geometric feature extraction. Application of a vessel mask removes the majority of false positives from vessels, while subsequent 3D region growing and geometric feature extraction will remove objects with large area, non-circular shape, or shifted centroid among multiple slices.

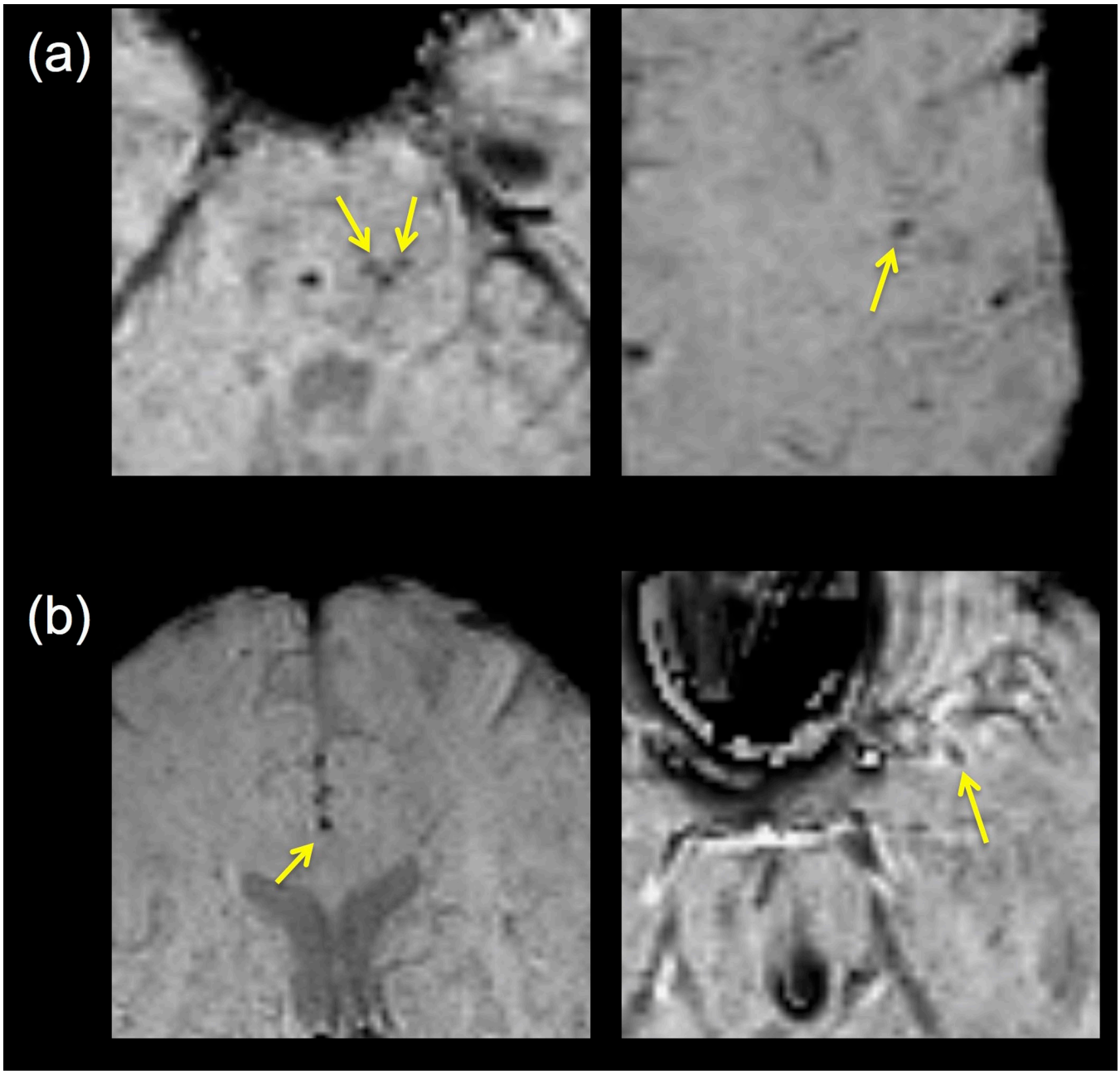

Fig. 2. Results of the adapted algorithm in the two training SWI scans

(a) 3 false negatives. **(b)** 2 representative false positives.

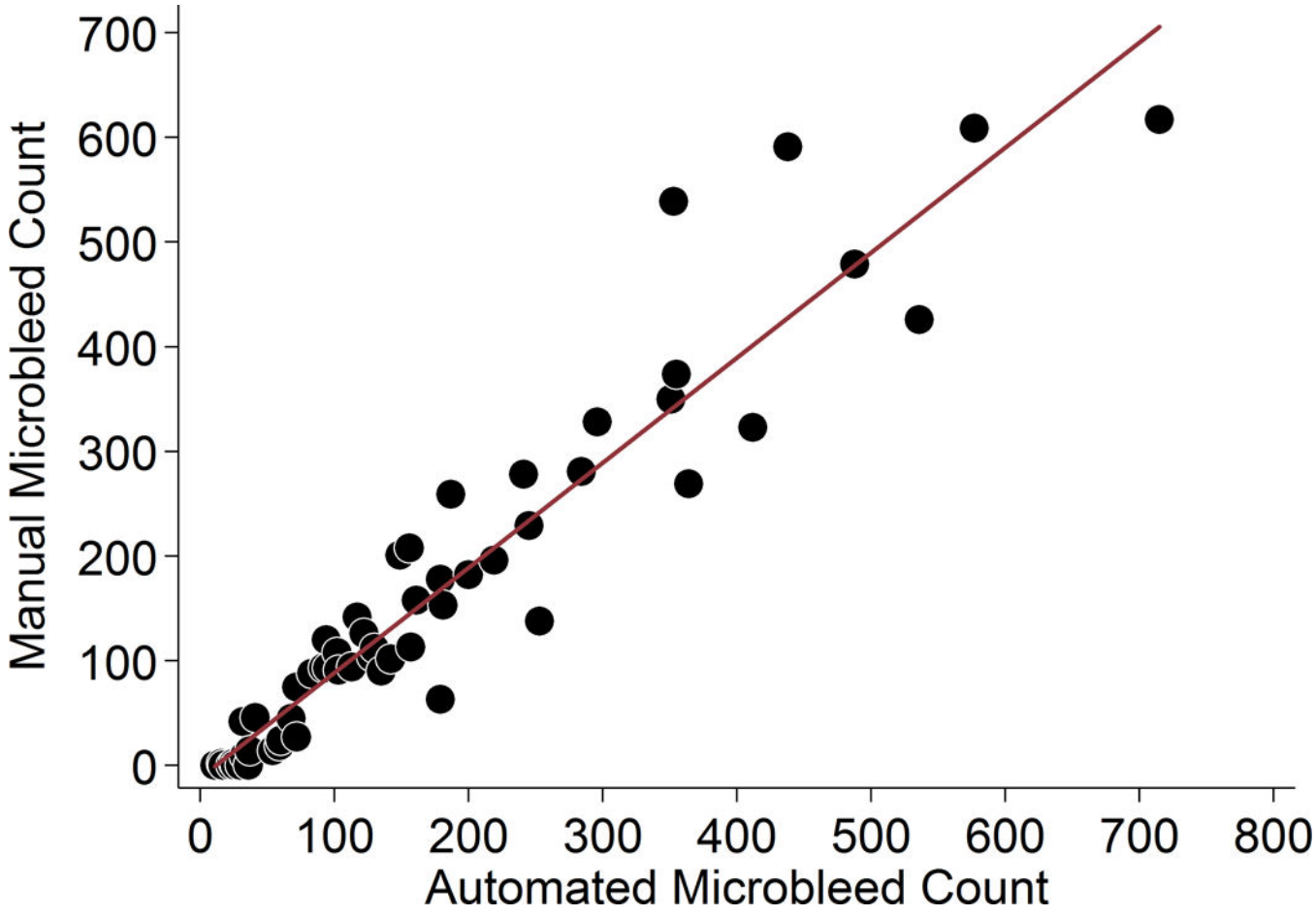

Fig. 3. Scatter plot of manual and automated microbleed counts for the 57 baseline scans

Linear regression $R^2 = 0.90$, $p < 0.001$. Intra-class r = 0.95, 95% CI = 0.91–0.97, $p < 0.001$. Paired t-test p = 0.11.

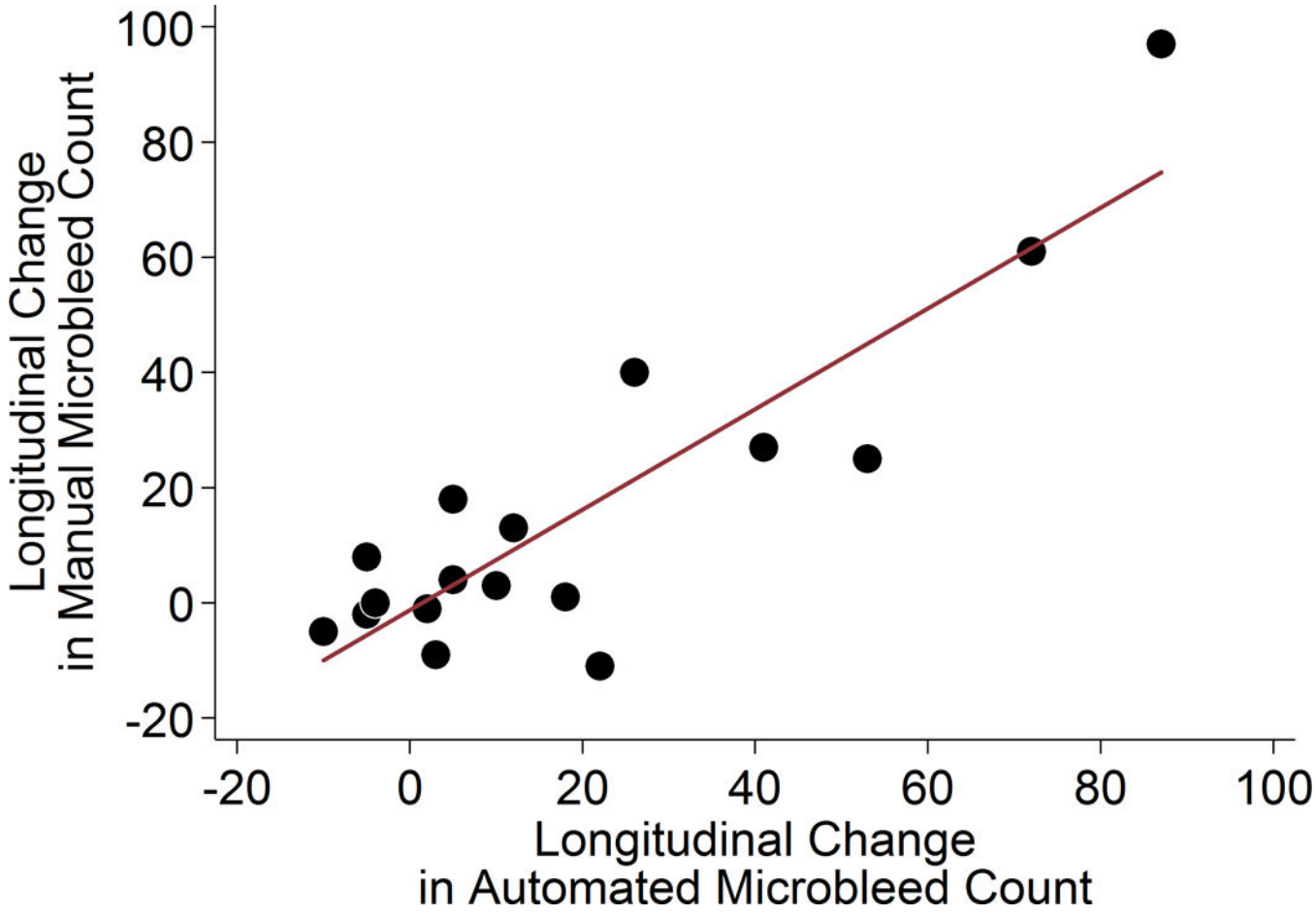

Fig. 4. Scatter plot of longitudinal changes in manual and automated microbleed counts in 17 patients

Time interval between baseline and follow-up scans was 39.4 +/− 5.3 months. Linear regression $R^2 = 0.76$, $p < 0.001$. Intra-class r = 0.87, 95% CI = 0.70–0.95, $p < 0.001$. Paired t-test p = 0.29.

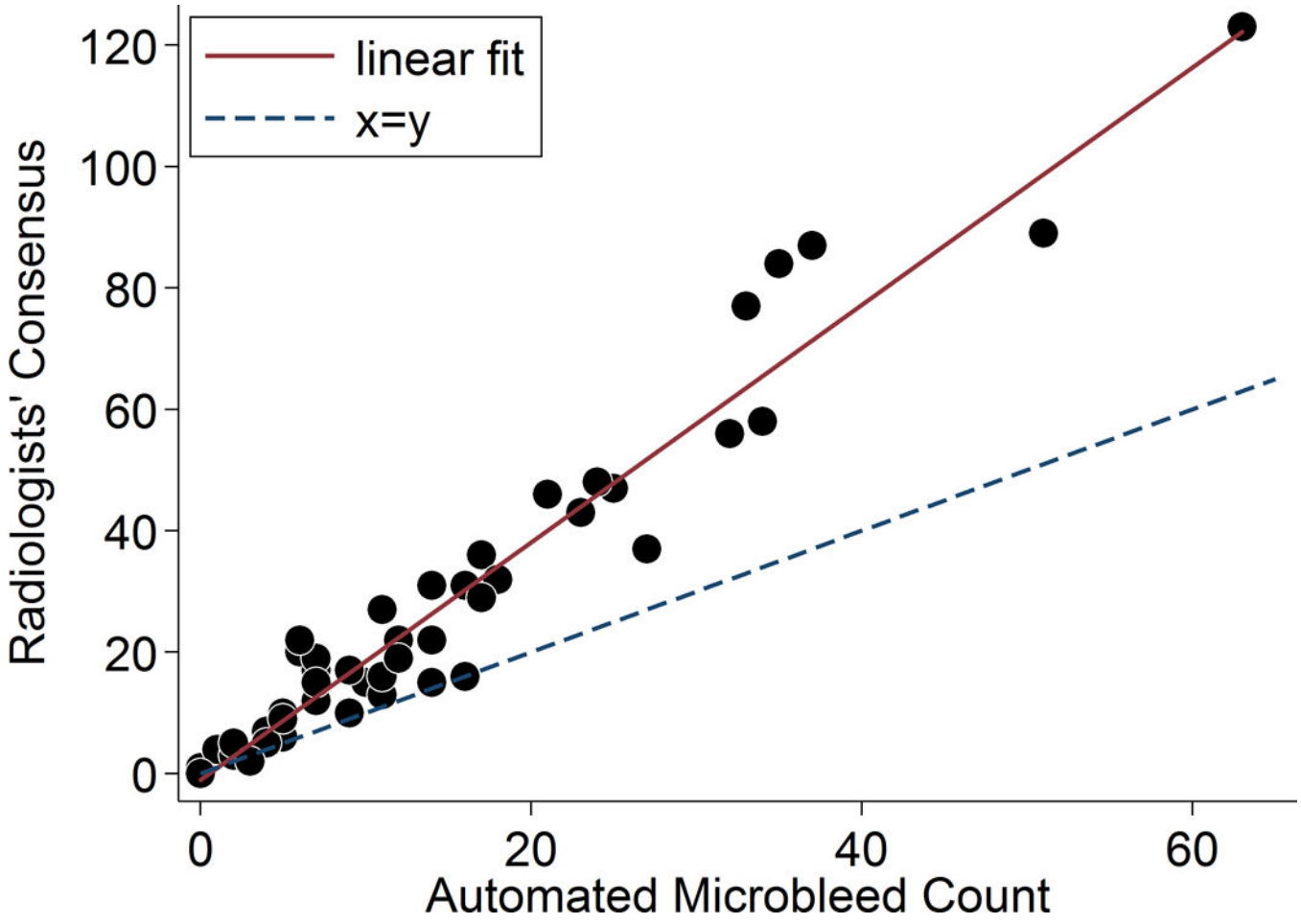

Fig. 5. Scatter plot of radiologists' consensus and automated microbleed counts on a selected slice from 47 patients (validation analysis)

Linear regression $R^2 = 0.94$, $p<0.001$. Intra-class r = 0.77, 95% CI = 0.62 – 0.87, $p<0.001$.

Table 1

Clinical characteristics of 57 CCM subjects at baseline

Age at baseline (mean ± sd)	50.1 ± 19.9
Female, n (%)	40 (70%)
History of clinical hemorrhage, n (%)	21 (37%)
History of seizures, n (%)	19 (33%)
History of headaches, n (%)	32 (56%)
Manual microbleed counts, median (min-max)	108 (0–617)